Novel Pyrene-Containing Organophosphates as Fluorescent Probes for Studying Aging-Induced Conformational Changes in Organophosphate-Inhibited Acetylcholinesterase†

G. Amitai,* Y. Ashani,* A. Gafni,* and I. Silman*

ABSTRACT: Aging of (substituted phosphoyl)–acetylcholinesterase conjugates, involving dealkylation of the bound substituted phosphoyl group, renders acetylcholinesterase resistant to reactivation by pyridine-2-aldoxime methiodide and other nucleophiles. Novel fluorescent organophosphates were synthesized and characterized which were designed to produce fluorescent (substituted phosphoro)–acetylcholinesterase conjugates corresponding to both the nonaged and aged forms. 1-Pyrenebutyl ethyl phosphorochloridate and 1-pyrenebutyl phosphorodichloridate both react rapidly and specifically with purified electric eel AChE to yield stoichiometric conjugates. The former produces a nonaged acetylcholinesterase conjugate which is readily reactivated by pyridine-2-aldoxime methiodide; the latter forms an aged conjugate which cannot be reactivated. There is no difference in the wavelengths of excitation and emission maxima of the two conjugates, but the quantum yield of fluorescence in the nonaged conjugate is reduced by ~50% compared to the aged conjugate. For both conjugates fluorescence decay measurements yield a decay curve which can be fitted by a three-component mechanism. The two slower decay components are shorter for the nonaged than for the aged conjugate. From these data the relative quantum yield of the nonaged form can be calculated to be ~60% of that of the aged conjugate, in agreement with the quantum yield derived from steady-state measurements, indicating that the quenching is primarily dynamic. Collisional quenching measurements showed that quenching of the bound pyrene by nitromethane obeys the Stern–Volmer equation for both conjugates, but the dynamic quenching constant for the nonaged conjugate is 1.6-fold higher than that for the aged conjugate. The spectroscopic data suggest that a possible explanation for the resistance to reactivation of the aged conjugate is that the substituted phosphoro group in this conjugate is more deeply buried inside the active site than in its nonaged counterpart.

Many serine hydrolases are inhibited irreversibly by organophosphates which react rapidly and specifically in a covalent reaction with the active-site serine of such enzymes (Aldridge & Reiner, 1972). The inhibited enzymes can often be reactivated by treatment of the (substituted phosphoyl)–enzyme conjugate with suitable nucleophilic reagents which detach the phosphoyl group from the serine hydroxyl (Wilson & Ginsburg, 1955; Childs et al., 1955; Cohen & Erlanger, 1960). However, in several such substituted phosphoyl enzymes, a process has been described, which is called aging, by which the inhibitor–enzyme conjugate is spontaneously converted to a form which can no longer be reactivated (Hobbiger, 1955).

Inhibition of acetylcholinesterase (acetylcholine acetylhydrolase, EC 3.1.1.7; AChE)[1] is the primary reason for the lethal action of many organophosphates, and to counter this toxic action a variety of quaternary oximes such as pyridine-2-aldoxime methiodide (2-PAM) have been developed which serve as active-site-directed reactivators of the inhibited enzyme (Froede & Wilson, 1971). The inability to regenerate aged (substituted phosphoyl)–AChE conjugates with such oximes renders the therapy of intoxication with certain organophosphates notoriously difficult (Loomis & Salafsky, 1963).

Evidence in the literature (Michel, 1958; Berends et al., 1959; Sun et al., 1979) indicates that aging of organophosphate-inhibited AChE commonly involves acid-catalyzed dealkylation of the substituted phosphoyl moiety, resulting in introduction of an O^- negative charge into the active site:

$$\underset{\text{free enzyme}}{EH} + XP(O)R(OR') \longrightarrow \underset{\text{inhibited enzyme}}{EP(O)R(OR')} \longrightarrow \underset{\text{aged enzyme}}{EP(O)R(O^-)}$$

R is usually an alkyl or alkoxy group, R′ is an alkyl group, and X is a leaving group (e.g., F, Cl, and *p*-nitrophenol). (Substituted phosphoyl)–enzyme conjugates in which R′ is a secondary or tertiary alkyl group age particularly rapidly by this route, which appears to proceed by an S_N1 mechanism, via a carbonium ion intermediate (Benschop & Keijer, 1966; Michel et al., 1967; Keijer et al., 1974). Aging may also occur by a second mechanism involving base-catalyzed P–O bond cleavage (Aldridge, 1975) which also seems to yield a negatively charged phosphoyl group like that obtained by dealkylation. In addition, aged phosphoyl–enzyme conjugates are obtained by inhibition of AChE with alkyl or aryl phosphorodichloridates (Wins & Wilson, 1974) or with predealkylated organophosphates such as desethyl Amiton (Aharoni & O'Brien, 1968) and methyl-1-(*S*-methylphosphoryl-3)-imidazolium (Chabrier & Jacob, 1980). In the case of the phosphorodichloridates, almost instantaneous aging is apparently produced as a result of nucleophilic substitution by OH^- of the chlorine atom not directly involved in reaction of the organophosphate with AChE (Wins & Wilson, 1974). In the two latter cases of predealkylated inhibitors, the inhibition

† From the Israel Institute for Biological Research (G.A. and Y.A.), Ness-Ziona, Israel, and the Departments of Neurobiology (I.S.) and Chemical Physics (A.G.), Weizmann Institute of Science, Rehovot, Israel. *Received August 3, 1981.*

[1] Abbreviations: AChE, acetylcholinesterase; 2-PAM, pyridine-2-aldoxime methiodide; PBEPC, 1-pyrenebutyl ethyl phosphorochloridate; PBPDC, 1-pyrenebutyl phosphorodichloridate; Nbs_2, 5,5′-dithiobis(2-nitrobenzoic acid); DEPF, diethyl phosphorofluoridate; NMR, nuclear magnetic resonance; MS, mass spectrometry; TLC, thin-layer chromatography; EPDF, ethyl phosphorodifluoridate; PBOH, 1-pyrenebutanol; PBEPF, 1-pyrenebutyl ethyl phosphorofluoridate; PBEP, *O*-(4-pyrenebutan-1-yl)ethoxyphosphoryl; PBP, *O*-(4-pyrenebutan-1-yl)hydroxyphosphoryl.

0006-2960/82/0421-2060$01.25/0

reaction itself introduces a substituted phosphoro moiety bearing a negative charge into the active site. Thus in all cases reported, whatever the mechanism, the aged (substituted phosphoyl)–AChE is assumed to contain an O^- negative charge in the active site. It has been suggested that this negative charge imposes an electrostatic barrier to the nucleophilic attack on the phosphorus atom by the oximate anion of the reactivator (Fleisher et al., 1967). Indeed, nonenzymic studies on the kinetics of reaction of neutral and negatively charged organophosphates with neutral and negatively charged nucleophiles (Kirby & Younas, 1970; Behrman et al., 1970a,b) indicate that the negative charge would retard reactivation; it would not, however, do so to an extent which could explain the complete failure to detect, experimentally, any reactivation of aged (substituted phosphoyl)–AChE conjugates by either oximes (Berends et al., 1959; Michel et al., 1967) or neutral nucleophiles such as amines (Sterri, 1977).

A possible explanation for the observed resistance to reactivation might be the occurrence of a conformational change as a result of the aging reaction. Fluorescent probes are particularly suitable for detecting such changes (Stryer, 1968; Brand & Gohlke, 1972), and it was decided, therefore, to synthesize fluorescent organophosphates tailored to examine this possibility. As the fluorophore we chose the pyrene moiety, which is particularly suitable for such studies because of its excitation wavelength (~340 nm), which is well separated from the protein absorption region, its high quantum yield, ~0.7 (Turro, 1978), and the long excited state lifetime, of the order of 100 ns (Barrantes et al., 1975). A pyrene-containing organophosphonate has been recently employed by Berman & Taylor (1978) as a fluorescent probe for the active site of *Torpedo* AChE.

Rather than preparing a fluorescent organophosphate which would undergo dealkylation when bound to the AChE molecule, we chose to synthesize one compound which would be expected to form a stable (substituted phosphoro)–AChE conjugate which would not age and a second organophosphate which would instantaneously generate an aged conjugate on reaction with AChE. As the first compound we selected 1-pyrenebutyl ethyl phosphorochloridate (PBEPC); its AChE conjugate should age very slowly since primary alkyl moieties are poor leaving groups in the dealkylation reaction (Hobbiger, 1955; Sun et al., 1979). As the second compound we selected 1-pyrenebutyl phosphorodichloridate (PBPDC). It was predicted that this compound, like the dichloridates prepared by Wins & Wilson (1974), should yield a (substituted phosphoro)–enzyme which would age almost instantaneously due to hydrolytic detachment of the chlorine atom not involved in reaction with the enzyme. The two fluorescent organophosphates, PBEPC and PBPDC, should thus yield nonaged and aged fluorescent conjugates, respectively, as shown in Scheme I.

A third compound, 1-pyrenebutyl ethyl phosphorofluoridate (PBEPF), was designed for use in cholinesterase localization studies (Amitai et al., 1980a) since phosphorofluoridates are much more stable in aqueous media than the corresponding phosphorochloridates (Ashani et al., 1973). PBEPF might be expected to produce a nonaged *O*-(4-pyrenebutan-1-yl)ethoxyphosphoryl–AChE conjugate analogous to the nonaged conjugate produced by PBEPC (see below).

In the following we describe the synthesis and characterization of these fluorescent organophosphates and show that they are potent covalent inhibitors of AChE. We further present kinetic data showing that PBEPC and PBPDC both react stoichiometrically with AChE to yield nonaged and aged

Scheme I[a]

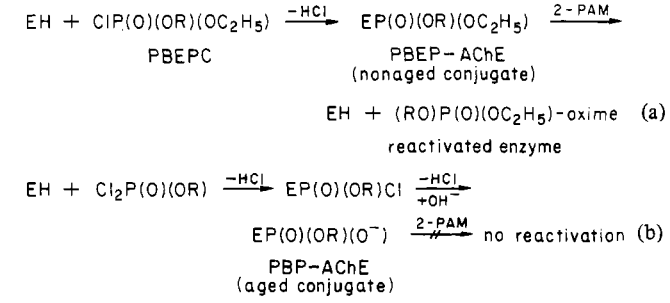

[a] R = 1-pyrenebutyl.

conjugates, respectively. Finally, we present steady-state and time-resolved fluorescence spectroscopy measurements showing distinct differences between the nonaged and aged conjugates. Some of these results have already been presented in preliminary communications (Amitai et al., 1979, 1980a,b).

Experimental Procedures

Materials. 5,5′-Dithiobis(2-nitrobenzoic acid) (Nbs_2) and pyridine-2-aldoxime methiodide (2-PAM) were obtained from Sigma Chemical Co. (St. Louis, MO); acetylthiocholine iodide was a product of Fluka, A.G. (Buchs, Switzerland); potassium iodide (Analar) and sodium thiosulfate (Analar) were from BDH Chemicals (Poole, England); nitromethane (spectral grade) was from Fischer Scientific Co. (Fair Lawn, NJ); Bio-Gel P-4 (100–200 mesh) was from Bio-Rad Laboratories (Richmond, CA). Salts and buffers were Analar grade. Pinacolyl methyl phosphonofluoridate (Soman) was prepared according to the procedure described by Monard & Quinchon (1961).

Diethyl phosphorofluoridate (DEPF) was prepared from diethyl phosphorochloridate (Aldrich Chemical Co., Milwaukee, WI) and sodium fluoride by the method of Saunders & Stacey (1948) and was more than 99% pure by gas chromatographic analysis. The 11S form of electric eel acetylcholinesterase (11S AChE; Dudai et al., 1972) was prepared according to Dudai & Silman (1974a).

Synthesis. Nuclear magnetic resonance (NMR) spectra were recorded on a Varian XL-100 spectrometer and interpreted principally according to Chapman & Magnus (1977). Mass spectrometry (MS) was performed on a Varian MAT-112 mass spectrometer. Melting points were determined on a Thomas melting point apparatus and were uncorrected. Microanalytical elemental analyses were performed by the Microanalytical Laboratories of the Hebrew University, Jerusalem. Thin-layer chromatography (TLC) was performed on glass plates (25 × 75 mm) coated with neutral silica without binder (Woelm, West Germany). Gas chromatography was performed by using a Hewlett-Packard Model 5700 apparatus equipped with a flame ionization detector.

The new fluorescent organophosphates were prepared according to the synthetic procedures outlined in Scheme II.

Ethyl Phosphorodifluoridate (EPDF). EPDF was prepared by reaction of the corresponding dichloridate (Aldrich Chemical Co., Milwaukee, WI) with 50% excess of NaF in dichlorobenzene. The product was distilled directly from the reaction mixture and redistilled through a Vigreux column (15 × 1 cm) under atmospheric pressure to give a colorless liquid: bp 80–81 °C [lit. bp 84–85 °C (Gold, 1961)]. EPDF is well characterized by its ^1H decoupled ^{31}P NMR spectrum: a triplet centered at δ −29 (relative to H_3PO_4) (J_{P-F} = 1000 Hz, which is a typical NMR spectrum for alkyl phosphorodifluoridates).

Scheme II

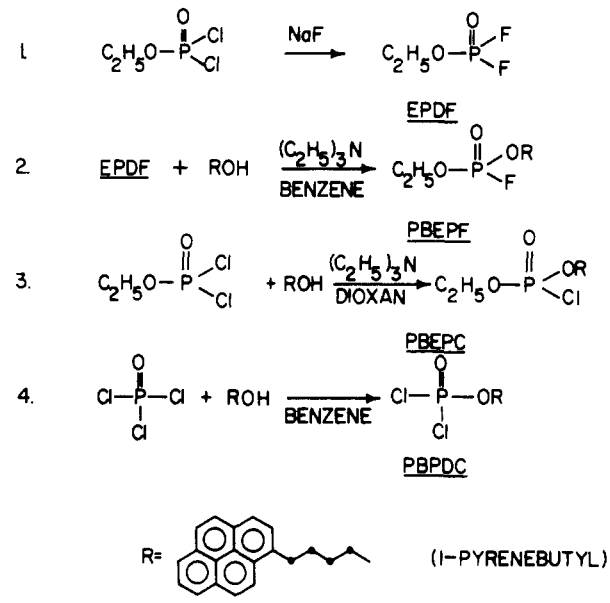

1-Pyrenebutanol (PBOH). PBOH was prepared by reducing 1-pyrenebutyric acid (Eastman Kodak, Rochester, NY) with lithium aluminum hydride. Our procedure is similar to that of Berman & Taylor (1978) except that the reaction was quenched with ethyl acetate and HCl instead of H_2O and NaOH. The crude product was purified on a Kieselgel 60 (Merck, Darmstadt, West Germany) column by elution with a mixture of benzene–ethyl acetate (9:1). The purified compound had a melting point of 75–76 °C [lit. mp (Berman & Taylor, 1978) 75–76.5 °C].

O-1-Pyrenebutyl O-Ethyl Phosphorofluoridate (PBEPF). A mixture of PBOH (2.7 g, 10 mmol) and triethylamine (1.3 g, 13 mmol) in 150 mL of benzene was added dropwise at room temperature to a solution of EPDF (1.6 g, 12 mmol) in 200 mL of dry benzene. The mixture was refluxed for 5 h and left overnight at room temperature. The white precipitate was filtered off and the solvent removed under reduced pressure. A white solid was obtained which recrystallized from light petroleum ether as white needles: mp 60–62 °C. Anal. Calcd for $C_{22}H_{22}O_3PF$: C, 68.75; H, 5.73. Found: C, 69.02; H, 5.59. The ^1H decoupled ^{31}P NMR spectrum revealed one doublet at δ −9.13 (relative to H_3PO_4) (J_{P-F} = 980 Hz). These data are characteristic of dialkyl phosphorofluoridates [$(RO)_2P(O)F$] where only one fluorine is attached to the phosphorus atom. A peak at m/z 384 was observed in the MS spectrum which equals the expected value for the molecular peak of PBEPF. TLC with ethyl acetate–chloroform (1:9) showed that recrystallized PBEPF is homogeneous (R_f 0.75).

O-1-Pyrenebutyl Phosphorodichloridate (PBPDC). A solution of PBOH (1.4 g, 5 mmol) in 50 mL of dry benzene was added dropwise to a solution of freshly distilled $POCl_3$ (3.8 g, 25 mmol) in 50 mL of dry benzene. This mixture was stirred overnight at room temperature, and the volatile constituents were removed under reduced pressure (1 mmHg) at 25 °C. The crude product was triturated with light petroleum ether (40–60 °C) and precipitated at 4 °C as a white solid: mp 52–54 °C (1.6 g, 40%). A single fluorescent spot (R_f 0.48) was noted under a UV lamp on a TLC plate using toluene–chloroform (3:2). The ^1H decoupled ^{31}P NMR spectrum (0.8 M in $CDCl_3$) revealed only one singlet at δ 6.6 (relative to H_3PO_4). Such a chemical shift is commonly ascribed to the phosphorus atom of monoalkyl phosphorodichloridates. The MS data showed a molecular peak at m/z 390, the expected value for PBPDC. Anal. Calcd for $C_{20}H_{17}PO_2Cl_2$: C, 61.38; H, 4.35. Found: C, 60.88; H, 4.86.

O-1-Pyrenebutyl O-Ethyl Phosphorochloridate (PBEPC). A mixture of PBOH (2.75 g, 10 mmol) and dry triethylamine (1.2 g, 12 mmol) in 10 mL of dry dioxane was added dropwise to a solution of ethyl phosphorodichloridate (3.2 g, 20 mmol) in dioxane at 5–7 °C. A yellow precipitate, which formed immediately, was filtered off after 1 h of stirring. The solvent and other volatile compounds were removed from the supernatant under reduced pressure (1–2 mmHg) at 25 °C to yield a green oil. The crude oil was purified on a Kieselgel 60 column using benzene–ethyl acetate (4:1) for elution, and the purified compound was obtained as a white solid (1 g, 25%): mp 74–76 °C. A single spot (R_f 0.70) was observed on a TLC plate using benzene–ethyl acetate (4:1). Anal. Calcd for $C_{22}H_{22}PO_3Cl$: C, 65.92; H, 5.63. Found: C, 67.00; H, 5.56. A molecular peak at m/z 400 was observed in the mass spectrum.

Acetylcholinesterase Activity Determinations. AChE activity and kinetics of inhibition and reactivation were monitored spectrophotometrically by the method of Ellman et al. (1961). The reaction mixture (3 mL) contained 0.4 mM acetylthiocholine iodide–0.3 mM Nbs_2–0.1 M NaCl–0.05% gelatin–0.01 M phosphate, pH 7.0, and measurements were performed at 25 °C.

Kinetics of Inhibition and Reactivation. Inhibition and reactivation kinetics were measured according to the methodology of Ashani & Leader (1979) (for details refer to Figure 3). The kinetic parameters for PBPDC were determined according to the procedure of Ashani et al. (1972).

Preparation of Fluorescent (Substituted Phosphoro)–AChE Conjugates for Spectroscopic Studies. Aliquots of 15 μL of either PBEPC or PBPDC (1.5×10^{-3} M in dry dioxane) were added portionwise to 1.5-mL samples of purified 11S AChE (0.8 mg/mL, $\sim 5 \times 10^{-6}$ M concentration of active sites) in 0.1 M NaCl–0.01 M phosphate, pH 7.0, yielding a final inhibitor concentration of 15 μM. After 10 min at 25 °C, both inhibitors reduced AChE activity >99%. The reaction mixtures were cooled to 0–2 °C in an ice–water bath and filtered immediately through a 6-mL Bio-Gel P-4 column at 4 °C. Fractions of 1 mL were collected, and the protein peak fractions (monitored at 280 nm) were retained at 4 °C until employed for spectroscopic measurements. In separate control experiments, AChE samples were first preincubated with the specific nonfluorescent AChE inhibitor, diethyl fluorophosphate (Wilson & Rio, 1965), at 1.5×10^{-6} M for 10 min at 25 °C. This treatment inhibited >99.5% of the AChE activity. These control samples were then treated with the fluorescent organophosphates and gel filtered as described above.

Spectroscopy. Spectrophotometric kinetic measurements utilized a Pye Unicam SP1800 double-beam spectrophotometer. Absorption spectra were measured in a Zeiss PMQ II spectrophotometer using fused silica cells (Hellma) of 1-cm path length. Fluorescence spectra were measured in a Perkin-Elmer MPF-3 spectrofluorometer using 1-cm optical path fluorescence cuvettes (Hellma). Fluorescence and absorption spectra were measured at 4 °C.

All spectroscopic measurements were performed in 0.1 M NaCl–0.01 M phosphate, pH 7.0. Absorption measurements were carried out at active-site concentrations of ~ 10 μM. For all fluorescence measurements, both steady state and time resolved, the active-site concentration was 0.5–0.7 μM.

Fluorescence Decay Measurements. Fluorescence decay measurements were performed with an instrument of the type described by Hundley et al. (1967), modified to overcome

Table I: Rates of Reaction of PBEPC, PBPDC, and PBEPF with Water and with AChE and Rates of Spontaneous Reactivation and Reactivation with 2-PAM of the Corresponding Phosphoro-AChE Conjugates[a]

inhibitor	$t_{1/2}$ (min)	k_h (min^{-1})	k_i (M^{-1} min^{-1})	k_r (min^{-1})	k_r' (min^{-1})
PBEPC	10	6.9×10^{-2}	4.6×10^{6}	3.7×10^{-3}	8.8×10^{-3}
PBPDC	0.08	8.7	2.6×10^{7}		
PBEPF	>100	$<6.9 \times 10^{-3}$	5.0×10^{5}	5.0×10^{-4}	8.0×10^{-3}
PBMPF			5.4×10^{6}	7.8×10^{-5}	4.2×10^{-3}
Soman	240	2.9×10^{-3}	1.8×10^{8}		

[a] All kinetic measurements, except those for PBMPF, were performed in 0.1 M NaCl-0.01 M phosphate, pH 7.0, at 25 °C. $t_{1/2}$ is the half-time for hydrolysis of the inhibitors; k_h is the first-order rate constant for hydrolysis, and k_i is the second-order rate constant for inhibition of electric eel 11S AChE. k_r is the first-order rate constant for spontaneous reactivation and k_r' the first-order rate constant for reactivation in the presence of 1 mM 2-PAM. The values of k_r and k_r' for PBEPF do not represent true kinetic constants since the reaction mixture contained residual PBEPF. The k_i value for PBEPC was obtained from the initial slope in Figure 2 where the level of hydrolysis of the inhibitor can be neglected. The values given for PBMPF are taken from Berman & Taylor (1978) who carried out their measurements in 0.1 M NaCl-0.041 M $MgCl_2$-0.01 M Tris, pH 8.0, 25 °C, using *Torpedo californica* 11S AChE.

problems due to drift which are associated with the repeated averaging procedures used in fluorescence decay measurements (Hazan et al., 1974).

Fluorescence decay curves were analyzed by using the method of nonlinear least squares (Grinvald & Steinberg, 1974), assuming the fluorescence decay mechanism to be a monoexponential or multiexponential function of the type $I(t) = \sum_i A_i \exp(-t/\tau_i)$ where $I(t)$ is the decay function and A_i and τ_i are the amplitude and lifetime of the ith component. $I(t)$ was convoluted with the time profile of the excitation pulse to give the calculated decay curve $F_c(t)$. The latter was compared with the experimental decay curve, $F(t)$, and the decay amplitudes and lifetimes were used as free parameters to be changed so as to minimize the value of the root mean square of the deviations between the calculated and experimental curves (RMS) defined as

$$\mathrm{RMS} = \left\{ \frac{1}{n} \sum_{i=1}^{n} [F_c(t_i) - F(t_i)]^2 \right\}^{1/2}$$

The summation is done over all n data points (for a typical experiment $n = 500$). The lifetime measurements were performed at 4 °C.

Results

Inhibition of AChE by the New Fluorescent Organophosphorus Esters. Table I summarizes the individual kinetic rate constants for inhibition by the new inhibitors and for their hydrolysis in water.

PBPDC, like other phosphorodichloridates (Wins & Wilson, 1974), showed the highest rates for both inhibition of AChE and for aqueous hydrolysis. Precise derivation of these constants for PBPDC necessitated, therefore, utilization of a kinetic procedure (Ashani et al., 1972) especially developed for such unstable organophosphates. The biomolecular rate constant for the inhibition of AChE by PBPDC can be calculated by use of (Ashani et al., 1972)

$$\ln \frac{E_t}{E_0} = -I_0 \frac{k_i}{k_h}(1 - e^{-k_h t}) \qquad (1)$$

where E_0 and E_t are the concentrations of active enzyme at zero time and time t, respectively, I_0 is the initial inhibitor concentration, k_i (M^{-1} min^{-1}) is the bimolecular rate constant for enzyme inhibition, and k_h (min^{-1}) is the pseudo-first-order rate constant for inhibitor hydrolysis. This equation extrapolates at infinite time to

$$\ln \frac{E_\infty}{E_0} = -I_0 \frac{k_i}{k_h} \qquad (2)$$

For a known concentration of inhibitor diluted directly into the enzyme solution (I_0), a constant value for ln (E_∞/E_0) is measured at infinite time, thus yielding k_i/k_h. In order to extract k_i from this expression, it is first necessary to determine k_h. This was done by using

$$I_{(\text{residual})} = I_{(\text{initial})}\, e^{-k_h t'} \qquad (3)$$

where in this case t' is the time of incubation of the unstable inhibitor in aqueous solution before its addition to the enzyme solution. The rate of decomposition of inhibitor is then expressed by the decrease in observed inhibition of AChE.

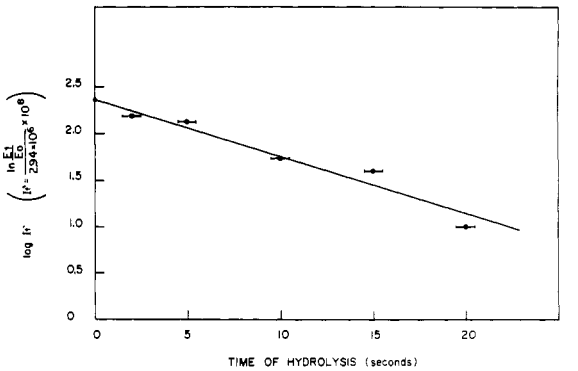

FIGURE 1: Determination of the hydrolysis rate constant, k_h, for PBPDC by measurement of the decrease in PBPDC concentration available for AChE inhibition, in accordance with eq 3 (see Results). The residual amount of the inhibitor ($I_{t'}$) was determined for each time period (t') of hydrolysis in the buffer without enzyme by substituting the corresponding values of ln $(E_\infty/E_0)_{t'}$ into eq 2. In this particular run we used the values I_0 (initial concentration) = 5×10^{-7} M and ln $(E_\infty/E_0)_0 = 1.47$. Thus the ratio k_i/k_h was calculated to be 2.94×10^6 M^{-1}. The factor of 10^8 has been introduced for convenience in presentation of the data.

Figure 1 shows a plot of residual activity for PBPDC dissolved in 0.1 M NaCl–0.01 M phosphate, pH 7.0, at 25 °C, as a function of the incubation time. As described above, the residual inhibitor concentration was determined by pipetting aliquots of this inhibitor solution, at the times given on the abscissa, into an AChE solution in the same buffer; enzymic activity was assayed after incubation with inhibitor for a sufficiently long time (>5 min) to assure complete hydrolysis of the PBPDC. The straight line obtained in Figure 1 thus represents the first-order-rate profile for the aqueous hydrolysis of PBPDC. From its slope one can calculate k_h (8.7 min^{-1}) and, as described above, thus obtain k_i (2.6×10^7 M^{-1} min^{-1}) for inhibition of AChE by PBPDC.

The bimolecular rate constants for inhibition of AChE by PBEPC and PBEPF, 4.6×10^7 and 5.0×10^5 M^{-1} min^{-1}, respectively, were determined by standard procedures. Under the experimental conditions employed (50–100-fold excess of inhibitor), the rates of inhibition by both compounds were

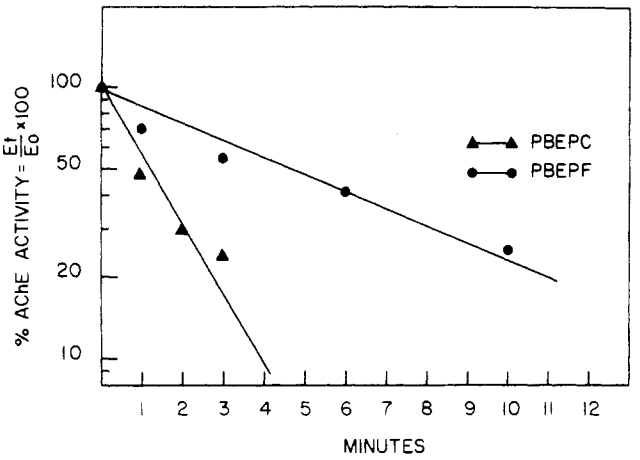

FIGURE 2: Kinetics of inhibition of AChE by PBEPC and PBEPF. Purified electric eel AChE ($\sim 10^{-9}$ M active sites) was incubated with either PBEPC (1.5×10^{-7} M) (▲) or PBEPF (2.8×10^{-7} M) (●) in 0.1 M NaCl–0.01 M phosphate, pH 7.0, at 25 °C. Residual activity, E_t/E_0, was measured at suitable times by assaying aliquots of the incubation mixture.

found to be first order and linearly related to the inhibitor concentration, as shown in Figure 2.

The decrease in the observed pseudo-first-order rate constant for enzyme inhibition, as a function of the time of preincubation of the inhibitor stock solutions, was used to calculate the rate constants for aqueous hydrolysis of PBEPC and PBEPF. As seen in Table I, PBEPF is considerably more stable than PBEPC: $t_{1/2} > 100$ min and $t_{1/2} = 10$ min, respectively. This is often the case when fluoridates are compared to the corresponding chloridates (Ashani et al., 1973); however, PBEPC itself is more stable than is usual for monochloridates (Wins & Wilson, 1974).

Reactivation of Fluorescent (Substituted Phosphoro)–Enzyme Conjugates. The kinetic constants for spontaneous reactivation and for induced reactivation with 2-PAM of the fluorescent (substituted phosphoro)–AChE conjugates are shown in Table I. As is the case for many (substituted phosphoyl)–AChE conjugates (Aldridge & Reiner, 1972), the conjugates obtained with PBEPC and PBEPF undergo fairly rapid spontaneous hydrolysis. Reactivation of enzyme inhibited with PBEPC occurs, at pH 7.0 and 25 °C, as a first-order reaction (Figure 3). Under the experimental conditions employed, it can be seen that the half-life of reactivation is ~3 h, and 97 ± 1% of the original enzymic activity is regained within 24 h. Incubation in the presence of 1 mM 2-PAM also leads to virtually complete reactivation. Here, too, first-order kinetics are observed (Figure 3), but the overall rate of reactivation is ~2.5-fold greater than that for spontaneous reactivation and is similar to that observed for PBMP–AChE in the presence of 2-PAM (Berman & Taylor, 1978). Both in the presence and in the absence of 2-PAM, the kinetic pattern of reactivation is consistent with the removal of a single homogeneous class of bound phosphoro groups. Although the 2-PAM-induced reactivation of AChE inhibited with PBEPF was carried out in the presence of a small residual amount of inhibitor, the kinetic constant, k_r', was found to be similar to that observed for enzyme inhibited with PBEPC. This suggests that the same (substituted phosphoro)–AChE species was produced by either PBEPF or PBEPC. However, when AChE was inhibited with PBPDC, no spontaneous or 2-PAM-induced reactivation whatsoever could be detected during periods of up to 48 h (Figure 3).

As can be seen in Figure 4, the rates of both spontaneous and 2-PAM-accelerated reactivation of PBEP–AChE display

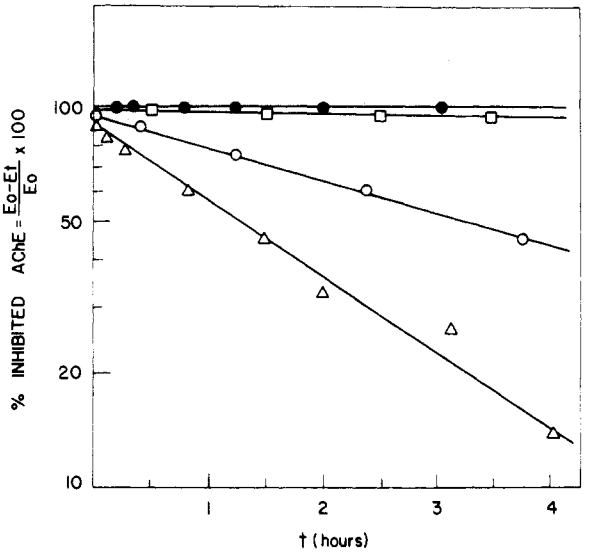

FIGURE 3: Kinetics of spontaneous and 2-PAM-induced reactivation of AChE inhibited with either PBEPC or PBPDC. AChE completely inhibited with PBEPC as described in Figure 2, or similarly inhibited with 2×10^{-7} M PBPDC, was diluted 100-fold into 0.1 M NaCl–0.01 M phosphate, pH 7.0, either in the presence or in the absence of 2-PAM and incubated at 4 or 25 °C. Reactivation was monitored by assaying aliquots of the reactivation mixtures at appropriate times. (△) Inhibition with PBEPC and reactivation at 25 °C in the presence of 1 mM 2-PAM; (○) inhibition with PBEPC and reactivation at 25 °C in the absence of 2-PAM; (□) inhibition with PBEPC and reactivation at 4 °C in the absence of 2-PAM; (●) inhibition with PBPDC and reactivation with 1 mM 2-PAM at 25 °C. The course of each reactivation process was monitored up to 48 h (not shown).

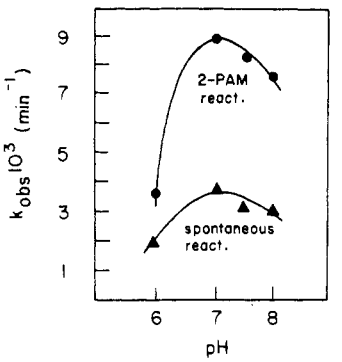

FIGURE 4: pH dependence of spontaneous and 2-PAM-induced reactivation of AChE inhibited by PBEPC. AChE (active-site concentration $\sim 10^{-7}$ M) was inhibited by incubation with 1×10^{-5} M PBEPC in 0.1 M NaCl–0.01 M phosphate, pH 7.0, at 25 °C, for 20 min, yielding complete inhibition. Aliquots of inhibited enzyme were diluted 100-fold, either into 1×10^{-3} M 2-PAM in 0.1 M NaCl–0.01 M phosphate at the appropriate pH value or into the same buffer in the absence of reactivator. At appropriate time intervals, aliquots were taken for enzymic assay. The figure shows the pseudo-first-order rate constants (k_{obsd}) thus obtained for spontaneous and 2-PAM-induced reactivation as a function of pH.

a bell-shaped pH dependence, with an optimum at pH 7.0, similar to those observed for other (substituted phosphoyl)–AChE conjugates (Hovanec & Lieske, 1972; Aldridge & Reiner, 1972).

In order to carry out detailed fluorescence measurements on the fluorescent (substituted phosphoro)–AChE conjugates, it was necessary to find conditions under which spontaneous reactivation was minimized. Although the rate of reactivation could be markedly diminished by lowering the pH (Figure 4), such conditions might accelerate acid-catalyzed aging (Aldridge & Reiner, 1972), and in fact only 85% of the initial AChE activity could be regained at pH 6. However, if the temperature was lowered to 4 °C, the rate of spontaneous

Table II: Fluorescence Decay Parameters and Relative Quantum Yields of PBEP-AChE, PBP-AChE, and PBPDC[a]

conjugate	A_1	τ_1	A_2	τ_2	A_3	τ_3	RMS[b]	$\frac{\Sigma A_i \tau_i}{\Sigma A_i}$[c]
PBP-AChE	0.849	0.58	0.053	39.9	0.098	114.4	0.0028	13.81
PBEP-AChE	0.903	0.66	0.057	17.6	0.039	102.0	0.0035	5.6
PBPDC[d]	0.132	17.5	0.868	87.3			0.0044	78.1

[a] All conditions are summarized in the legend to Figure 6. The life-times are expressed in nanoseconds. [b] RMS = root mean square of the deviations as defined under Experimental Procedures. [c] Relative quantum yield; see also Grinvald et al. (1975). [d] A 1 mM solution of PBPDC in dioxane was diluted 10^3-fold into 0.1 M NaCl–0.01 M phosphate, pH 7.0, so as to yield a 1 μM solution of free ligand, presumably in the corresponding acid form (the pyrenebutyl ester of phosphoric acid).

reactivation was greatly reduced (Figure 3), with the $t_{1/2}$ increasing to ~60 h. In all the spectral studies described below, therefore, the PBEP–AChE conjugate was maintained at 0–4 °C prior to and during measurements.

Specificity of Binding and Stoichiometry of (Substituted Phosphoro)–AChE Conjugates. In order to employ the fluorescent organophosphates as probes for detecting conformational changes which might occur during aging of (substituted phosphoro)–AChE conjugates, it was necessary to establish that they interact specifically and stoichiometrically with the enzyme. There is evidence from studies using either radioactive organophosphates (Froede & Wilson, 1970) or covalent AChE inhibitors which release a fluorophore on reaction with the active-site serine in the catalytic subunit (Gordon et al., 1978) that organophosphates do, indeed, react exclusively with the active-site serine in the catalytic subunit. Berman & Taylor (1978) showed this to be the case for PBMPF, the pyrene-containing organophosphate which they employed.

The specificity of binding of PBEPC and PBPDC to AChE was first investigated by preincubating electric eel 11S AChE with diethyl phosphorofluoridate (DEPF) before treatment with the fluorescent organophosphate. DEPF is known to react specifically with the active-site serine of AChE (Wilson & Rio, 1965); this pretreatment should, therefore, prevent binding of the fluorescent organophosphate. Incubation of AChE with 1.5 μM DEPF for 10 min at pH 7.0 and 25 °C inhibited 99.5% of the AChE activity. This incubation was followed by similar incubation with either 1.5 μM PBEPC or 1.5 μM PBPDC. The reaction mixture was then passed over a Bio-Gel P-4 column so as to separate the enzyme from free fluorescent organophosphates. The fluorescence of such an enzyme sample was compared with that of a sample of AChE similarly treated with PBEPC or PBPDC without pretreatment with DEPF, as described below. The fluorescence of the DEPF-treated samples was found to be <5% of that of the nontreated samples.

The above experiment provided strong evidence that the fluorescent organophosphates react specifically with the active-site serine of the catalytic subunits. The stoichiometry of binding was determined by measuring the absorption of the bound pyrene at 347 nm, the absorption maximum for pyrene in both conjugates (Figure 5), and the absorption of AChE at 280 nm (where the bound pyrene makes only a minor contribution to the total absorbance). The concentration of bound pyrene was determined assuming $\epsilon_{347} = 4 \times 10^4$ M^{-1} cm^{-1} (Knopp & Weber, 1969; Berman & Taylor, 1978), and the enzyme concentration was determined from the absorbance at 280 nm by using $A_{280}^{1\%} = 17.6$ (Dudai et al., 1972) and a molecular weight per catalytic subunit of 82 000 (Dudai & Silman, 1974b). From the ratios of ϵ_{347} to ϵ_{280}, it was calculated that there are 0.99 mol of bound pyrene per active site for the PBEP–AChE conjugate and 0.98 for the PBP conjugate. When known uncertainties with respect to the subunit molecular weight (Rosenberry, 1975) and to the extinction coefficients for both AChE (Rosenberry et al., 1972) and the bound pyrene are taken into account, it can be estimated that in both conjugates there are 0.85–1.15 molecules of bound pyrene per catalytic subunit. The two conjugates can, therefore, be employed for studying spectral differences between aged and nonaged substituted phosphoro conjugates.

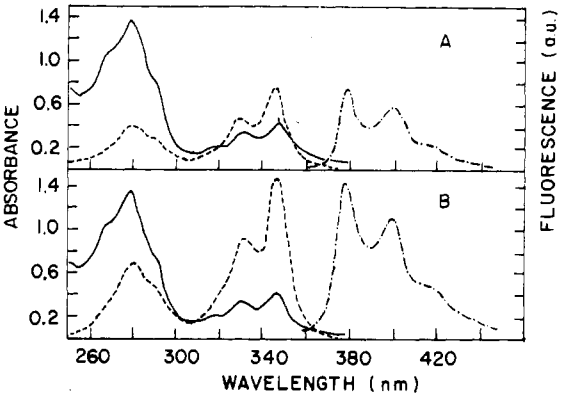

FIGURE 5: Absorption and fluorescence excitation and emission spectra of aged and nonaged conjugates of AChE. (A) Nonaged PBEP–AChE. (B) Aged PBP–AChE. Absorption spectra (—) were recorded at active-site concentrations of ~10.6 μM for PBEP–AChE and ~9.4 μM for PBP–AChE, and the spectra were corrected to equal concentrations of both conjugates. Fluorescence excitation (- - -) and emission (–·–) spectra were recorded at equal active-site concentrations of both conjugates: 0.7 μM. The conjugates were dissolved in 0.1 M NaCl–0.01 M phosphate, pH 7.0, and spectra were recorded at 3 °C.

Steady-State Fluorescence. The fluorescence emission and excitation spectra of nonaged PBEP–AChE and aged PBP–AChE are displayed alongside the corresponding absorption spectra in Figure 5. There is no difference in the wavelength of excitation and emission maxima for pyrene in PBEP–AChE and PBP–AChE. Moreover, in both conjugates the maxima for excitation correspond to the maxima of absorption (284, 330, and 347 nm). However, the fluorescence yield for pyrene in the nonaged conjugate, PBEP–AChE, is ~50% quenched compared to the aged conjugate, PBP–AChE (Figure 5). It is of interest that in both conjugates the principal absorption wavelength (347 nm) is shifted by 4 nm relative to that for the free chromophore (343 nm). Similar shifts were also observed by Berman & Taylor (1978) for PBMP–AChE by using the *Torpedo* enzyme (λ_{max} 349 nm) and for the pyrene moiety in the pyrenebutyric acid–bovine serum albumin complex (λ_{max} 345 nm) (Vaughn & Weber, 1970) and in the pyrenebutyrate–antipyrenebutyrate antibody complex (λ_{max} 347 nm) (Lovejoy et al., 1977).

Time-Resolved Emission Spectroscopy. Fluorescence decay curves for PBEP–AChE and PBP–AChE are displayed in Figure 6. For both conjugates a good fit for the fluorescence decay curve could only be obtained by assuming a three-component decay mechanism, with the decay constants being

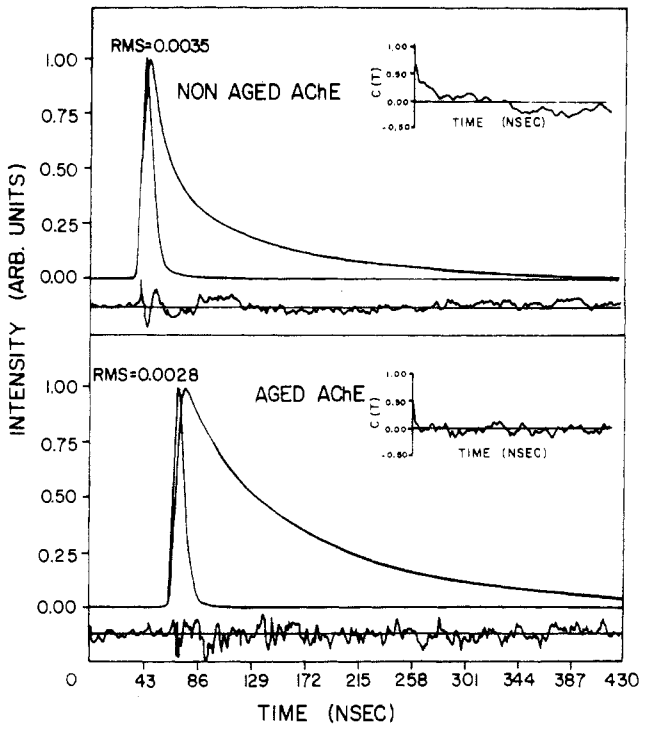

FIGURE 6: Fluorescence decay of the (substituted phosphoro)–AChE conjugates, PBEP–AChE and PBP–AChE. The decay data were obtained for equal concentrations (0.7 μM catalytic sites) of both conjugates in 0.1 M NaCl–0.01 M phosphate, pH 7.0, at 4 °C. The decay parameters are summarized in Table II. The traces of the deviations between the theoretical and experimental decay curves are shown below each curve, and the autocorrelation functions of the deviations are shown in the inset at the upper right: λ_{ex} = 347 nm; λ_{em} > 400 nm.

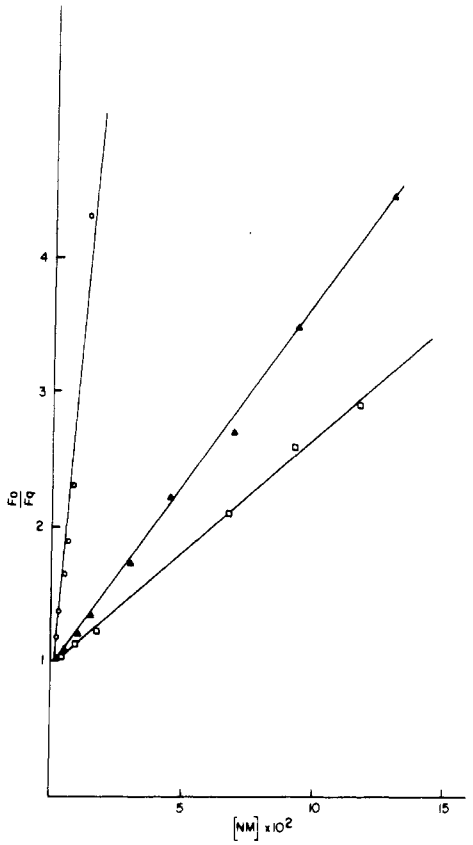

FIGURE 7: Stern–Volmer plots for the quenching by nitromethane of pyrene fluorescence in PBEP–AChE and PBP–AChE. F_0 is the fluorescence intensity without quencher, and F_q is the fluorescence intensity in the presence of quencher. The Stern–Volmer plots for pyrenebutanol (10^{-7} M) (○), PBEP–AChE (7×10^{-7} M) (▲), and PBP–AChE (7×10^{-7} M) (□) were measured in 0.1 M NaCl–0.01 M phosphate, pH 7.0, at 3 °C: λ_{ex} = 347 nm; λ_{em} = 380 nm.

given in Table II. The two longer decay components obtained in the analysis are both significantly longer for aged PBP–AChE, τ_2 = 39.7 ns and τ_3 = 114.4 ns, than for nonaged PBEP–AChE, τ_2 = 17.6 ns and τ_3 = 102.0 ns, whereas the values of the third short component in both cases are not significantly different, τ_1 = 0.58 ns and τ_1 = 0.66 ns, respectively.

Relative quantum yields can be calculated from values of $\sum_i A_i\tau_i/\sum_i A_i$ where τ_i and A_i, respectively, are the lifetime and amplitude for the ith component (Grinvald et al., 1975). Values calculated according to the above equation show a reduction of ~40% in the intensity of fluorescence emission for BPEP–AChE as compared to PBP–AChE, in agreement with the steady-state results (Figure 5). This agreement strongly indicates that the quenching of pyrene fluorescence in PBEP–AChE relative to PBP–AChE is primarily dynamic.

Intrinsic Fluorescence. The intrinsic protein fluorescence of 11S electric eel AChE originates primarily from the relatively large number of tryptophan residues; each catalytic subunit contains between 10 and 20 tryptophan residues, some of which appear to be in the close vicinity of the active site (Shinitzky et al., 1973; Goeldner & Hirth, 1980). Fluorescence emission intensities of the two conjugates (λ_{ex} 284 nm; λ_{em} 330 nm) were measured relative to the unmodified enzyme. Tryptophan fluorescence was markedly quenched in both conjugates, but more so in the "aged" conjugate, PBP–AChE. Thus PBP–AChE was 5-fold quenched relative to free AChE, whereas PBEP–AChE was only 3-fold quenched. The quenching of tryptophan emission probably stems from energy transfer (Forster, 1959) from tryptophan residue(s) to the covalently bound pyrene moiety. This conclusion is supported by measurement of the intrinsic fluorescence of AChE inhibited with Soman, an aliphatic organophosphonate with potent anticholinesterase activity (Table I), whose absorption bands do not overlap the tryptophan emission bands. Incubation of 11S AChE with 5×10^{-8} M Soman for 10 min at pH 7.0 and 25 °C inhibited AChE activity >99% but reduced the intrinsic fluorescence by less than 10%. Control experiments in which 5×10^{-8} M fluoride alone was added to an AChE solution suggested that most of this quenching was due to interaction of free fluoride with the enzyme.

Collisional Quenching. Dynamic collisional quenching of pyrene fluorescence by iodide and nitromethane was measured for PBEP–AChE, PBP–AChE, and the free fluorophore pyrenebutanol (PBOH). The Stern–Volmer plots obtained for iodide and nitromethane are depicted in Figures 7 and 8, respectively. The values for the dynamic quenching constant, K_Q, were found to be, in the case of iodide, 3.0 and 3.2 M^{-1} for the nonaged and aged conjugates, respectively. When nitromethane was the quencher, K_Q values of 27 and 17 M^{-1} were observed for the nonaged and aged enzymes, respectively. The constant (K_Q) for quenching of the free fluorophore by both iodide (46 M^{-1}) and nitromethane (182 M^{-1}) is greater by at least 1 order of magnitude than that obtained for the bound pyrene in both conjugates (Figures 7 and 8), in agreement with the results of Berman & Taylor (1978). All Stern–Volmer plots were linear in the concentration range employed (0.005–0.08 M for I^-; 0.005–0.13 M for nitromethane). The value of K_Q for nitromethane colliding with the pyrene moiety in the PBEP–AChE conjugate is thus 1.6-fold larger than that obtained for PBP–AChE, while the values of K_Q for I^- for both conjugates are similar, yet much smaller than those obtained for nitromethane.

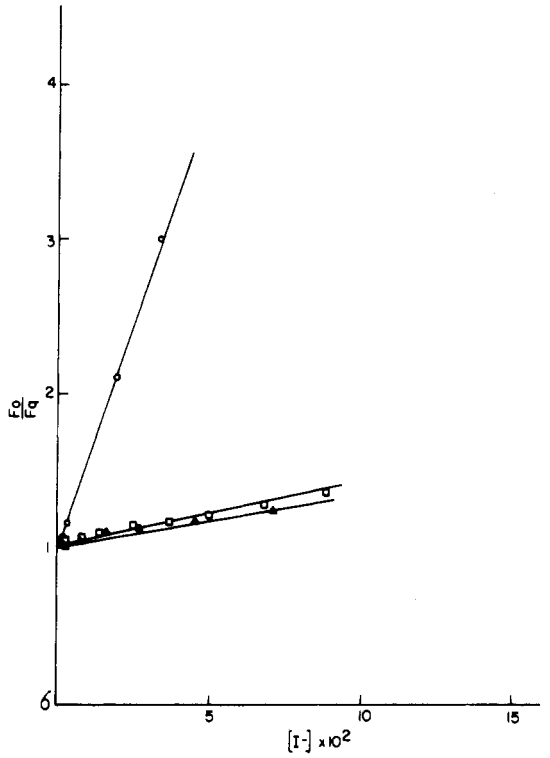

FIGURE 8: Stern–Volmer plots for the quenching by iodide of pyrene fluorescence in PBEP–AChE and PBP–AChE. F_0 and F_q are the same as in Figure 7. The plots for pyrenebutanol (○), PBEP–AChE (▲), and PBP–AChE (□) were obtained at the same concentrations and under the same experimental conditions as described in Figure 7. The measurements employed potassium iodide in the presence of 1 mM sodium thiosulfate.

Stern–Volmer plots for the quenching of the tryptophan fluorescence of 11S AChE and of the conjugates PBEP–AChE and PBP–AChE by nitromethane are depicted in Figure 9. All the plots deviate markedly from linearity. This is to be expected (Lehrer & Leavis, 1978) in view of the large number of tryptophan residues (10–20) in each catalytic subunit of electric eel AChE (Shinitzky et al., 1973). While the differences between the Stern–Volmer plots for PBEP–AChE and PBP–AChE are small, a marked difference was obtained between these curves and that obtained for the unmodified enzyme.

Iodide ions were found to be much less efficient quenchers of tryptophan fluorescence, as of pyrene fluorescence. As can be seen in Figure 9, identical Stern–Volmer plots are obtained for the free enzymes and for the two organophosphorus conjugates.

Discussion

The fluorescent organophosphates which we prepared were designed to produce models of aged and nonaged (substituted phosphoro)–AChE conjugates. Indeed, they were found to react rapidly (at rates comparable to commonly employed organophosphorus inhibitors) and specifically with electric eel AChE. In accordance with our expectations PBEPC and PBPDC produced nonaged and aged conjugates, respectively, with the former being totally reactivatable by 2-PAM and the latter completely resistant.

The various spectroscopic measurements presented under Results all reveal significant differences between the "aged" and "nonaged" conjugates which imply that aging has modified the environment of the pyrene chromophore as well as of tryptophan residue(s) in the AChE molecule.

It was necessary, in the time-resolved fluorescence experiments, for both conjugates to assume a three-exponential decay

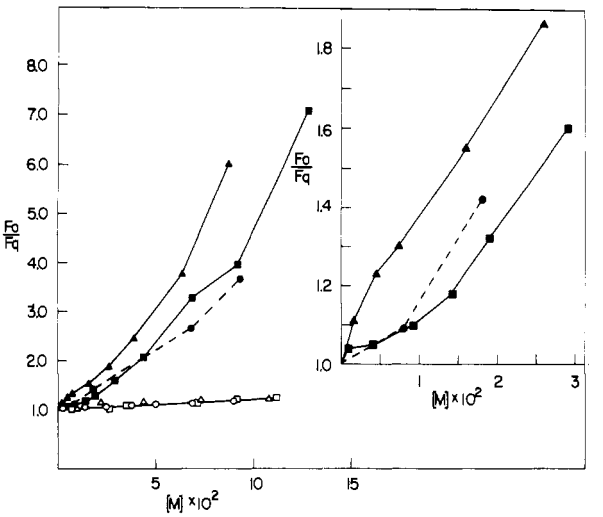

FIGURE 9: Stern–Volmer plots for the quenching of tryptophan fluorescence by nitromethane and by iodide. Quenching of fluorescence by nitromethane was measured for unmodified AChE (▲), PBEP–AChE (●), and PBP–AChE (■). The quenching by iodide was measured for unmodified AChE, (△), PBEP–AChE (○), and PBP–AChE (□) in the presence of 1 mM sodium thiosulfate. All other conditions were as in Figures 7 and 8. The inset (upper right) presents the quenching data with nitromethane in the lower concentration ranges using an expanded scale.

mechanism in order to obtain a good fit between calculated and experimental decay curves. The two longer components were found to differ significantly for the two conjugates, indicating that the quenching of pyrene fluorescence observed in the steady-state fluorescence of the nonaged conjugate PBEP–AChE, relative to the aged conjugate PBP–AChE, is primarily dynamic (Table II). Thus, quenching of steady-state fluorescence is ~50%, and a value of ~60% can be calculated from the fluorescence decay data. The very short component, τ_1, assumes very similar values for both conjugates (0.58 ns for PBP–AChE and 0.66 ns for PBEP–AChE). This component does not originate in light-scattering or other instrumental artifacts, since free 11S AChE alone gave no detectable signal under the identical conditions used to collect lifetime data for the (substituted phosphoro)–AChE conjugates. The free organophosphate, PBPDC, in solution, which is, in fact, in its phosphate form due to rapid hydrolysis, reveals a two-exponent decay mechanism (Table II). This suggests that the short component observed for both (substituted phosphoro)–AChE conjugates stems from putative interactions between the probe and the enzyme. Berman et al. (1980) found only two-component decay for the conjugate formed by PBMPF with 11S AChE from *Torpedo*. These authors did not, however, deconvolve the decay curve in order to eliminate the distortions in the first few nanoseconds due to the finite width of the lamp flash.

The data for collisional quenching of pyrene fluorescence by nitromethane and iodide (Figures 7 and 8) show that for both quenchers the chromophore is much less accessible in the (substituted phosphoro)–AChE conjugates than when free in solution. Furthermore, quenching by nitromethane in both conjugates is much more efficient than that by iodide. The low accessibility of I^- in both conjugates is consistent with the presence of a hydrophobic region, situated close to the pyrene moiety, favoring the entrance of neutral molecules such as nitromethane and limiting the approach of negatively charged iodide ions (Berman & Taylor, 1978). The fact that nitromethane is a more efficient quencher of the pyrene in PBEP–AChE than in PBP–AChE implies that the pyrene fluorophore in the aged conjugate is less accessible to nitro-

methane than in its nonaged counterpart.

For collisional quenching of tryptophan fluorescence, also, iodide is much less efficient than nitromethane (Figure 9). As was the case for the pyrene fluorophore, the polar iodide ion has difficulty in penetrating the nonpolar regions in which the fluorescing residues reside. It is of interest to note a significant difference in dynamic quenching of tryptophan by nitromethane between free enzyme and the two conjugates and, to a lesser degree, between the two conjugates themselves. Because the presence of pyrene causes extensive quenching of tryptophan in both conjugates (~5-fold for the aged conjugate and 3-fold for the nonaged conjugate), it is difficult to ascribe significance to the differences observed in dynamic quenching by nitromethane.

The most probable explanation for the observed differences in fluorescent parameters between the aged and nonaged conjugates is a conformational change resulting from the aging process. However, a change in the spatial orientation of the pyrene group relative to its binding site, due to a conformational change in the substituted phosphoro moiety which does not involve corresponding movement in the enzyme itself, must also be considered. Since our experimental data suggest that quenching is primarily dynamic, the former possibility is favored. In both the aged and nonaged conjugates the pyrene fluorophore should be relatively exposed to the external medium compared to the phosphorus function; the differences in fluorescent parameters observed may, therefore, reflect an even greater change in the accessibility of the phosphorus atom to the nucleophilic reactivator. Thus the total resistance of the aged enzyme to reactivation may involve the combined effects of diminished accessibility due to a conformational change and the electrical factors referred to in the introduction. The pyrene moiety, despite its many virtues as a fluorescent probe, is relatively insensitive to environment with respect to both quantum yield and shifts in the wavelength of absorption and emission (Birks, 1970). Indeed, we observed no difference in absorption and emission maxima between PBP–AChE and PBEP–AChE. In order to seek additional information concerning the environment of the chromophore in the aged and nonaged conjugates, it will be desirable, in the future, to prepare similar fluorescent conjugates containing such fluorophores as the dansyl moiety which are more sensitive to the environment [see, for example, Epstein et al. (1979)].

Various quaternary ligands and metal ions specific for the catalytic and peripheral anionic binding sites of AChE have been shown to enhance or retard acylation and phosphorylation of the enzyme by substrates and inhibitors (Rosenberry, 1975). More recently, Tomlinson et al. (1980) demonstrated that Ca^{2+}, Mg^{2+}, gallamine, and propidium accelerate carbamoylation as well as decarbamoylation of dimethylcarbamoyl–AChE, whereas Zn^{2+} and *d*-tubocurarine decrease the carbamoylation amplitude. These results support, in general, the two-state model proposed by Pattison & Bernhard (1978) for *Torpedo* enzyme in which peripheral ligands alter the distributions of the two states. In addition, a number of in vitro studies have shown that certain quaternary ligands may retard or enhance the aging process after inhibition of AChE by Soman (Schoene, 1978) or by Sarin (Crone, 1974). A possible approach to reactivation of aged (substituted phosphoyl)–AChE conjugates may thus involve a search for suitable quaternary ligands which might reverse the putative conformational change in the aging process for which we have provided experimental evidence.

Acknowledgments

We thank Dr. Shmaryahu Blumberg and Dr. Meir Shinitzky for valuable discussions.

References

Aharoni, A. H., & O'Brien, R. D. (1968) *Biochemistry 7*, 1538–1545.

Aldridge, W. N. (1975) *Croat. Chem. Acta 47*, 215–233.

Aldridge, W. N., & Reiner, E. (1972) *Enzyme Inhibitors as Substrates*, Elsevier, Amsterdam.

Amitai, G., Ashani, Y., Shahar, A., & Silman, I. (1979) *Abstr. Meet. Int. Soc. Neurochem. Jerusalem, 7th*, 192.

Amitai, G., Ashani, Y., Shahar, A., Gafni, A., & Silman, I. (1980a) *Monogr. Neural Sci. 7*, 70–84.

Amitai, G., Ashani, Y., Gafni, A., & Silman, I. (1980b) *Neurochem. Int. 2*, 199–204.

Ashani, Y., & Leader, H. (1979) *Biochem. J. 177*, 781–790.

Ashani, Y., Wins, P., & Wilson, I. B. (1972) *Biochim. Biophys. Acta 284*, 427–434.

Ashani, Y., Snyder, S. L., & Wilson, I. B. (1973) *J. Med. Chem. 16*, 446–450.

Barrantes, F. J., Sakmann, B., Bonner, R., Eibl, H., & Jovin, T. M. (1975) *Proc. Natl. Acad. Sci. U.S.A. 72*, 3097–3101.

Behrman, E. J., Biallas, M. J., Brass, H. J., Edwards, J. O., & Isaks, M. (1970a) *J. Org. Chem. 35*, 3063–3069.

Behrman, E. J., Biallas, M. J., Brass, H. J., Edwards, J. O., & Isaks, M. (1970b) *J. Org. Chem. 35*, 3069–3075.

Benschop, H. P., & Keijer, J. H. (1966) *Biochim. Biophys. Acta 128*, 586–588.

Berends, F., Posthumus, C. H., Sluys, I. V. D., & Deierkauf, F. (1959) *Biochim. Biophys. Acta 34*, 576–578.

Berman, H. A., & Taylor, P. (1978) *Biochemistry 17*, 1704–1713.

Berman, H. A., Yguerabide, J., & Taylor, P. (1980) *Biochemistry 19*, 2226–2235.

Birks, J. B. (1970) *Photophysics of Aromatic Molecules*, pp 128–129, Wiley-Interscience, New York.

Brand, L., & Gohlke, J. R. (1972) *Annu. Rev. Biochem. 41*, 843–868.

Chabrier, P. E., & Jacob, J. (1980) *Arch. Toxicol. 45*, 15–20.

Chapman, O., & Magnus, P. D. (1977) *Introduction to Practical High Resolution NMR Spectroscopy*, p 108, Academic Press, New York.

Childs, A. F., Davies, A. R., Green, A. L., & Rutland, J. P. (1955) *Br. J. Pharmacol. 10*, 462–465.

Cohen, W., & Erlanger, B. F. (1960) *J. Am. Chem. Soc. 82*, 3928–3934.

Crone, H. D. (1974) *Biochem. Pharmacol. 23*, 460–462.

Dudai, Y., & Silman, I. (1974a) *Methods Enzymol. 34*, 571–580.

Dudai, Y., & Silman, I. (1974b) *Biochem. Biophys. Res. Commun. 59*, 117–125.

Dudai, Y., Silman, I., Kalderon, N., & Blumberg, S. (1972) *Biochim. Biophys. Acta 268*, 138–157.

Ellman, G. L., Courtney, K. D., Andres, V., & Featherstone, R. M. (1961) *Biochem. Pharmacol. 7*, 88–95.

Epstein, D., Berman, H. A., & Taylor, P. (1979) *Biochemistry 18*, 4749–4754.

Fleisher, J. H., Harris, L. W., & Murtha, E. F. (1967) *J. Pharmacol. Exp. Ther. 156*, 345–351.

Forster, Th. (1959) *Discuss. Faraday Soc. 27*, 7–17.

Froede, H. C., & Wilson, I. B. (1970) *Isr. J. Med. Sci. 6*, 179–184.

Froede, H. C., & Wilson, I. B. (1971) *Enzymes, 3rd Ed. 5*, 87–114.

Goeldner, M. P., & Hirth, C. G. (1980) *Proc. Natl. Acad. Sci. U.S.A. 77*, 6439–6442.

Gold, A. M. (1961) *J. Org. Chem. 26*, 3991–3994.

Gordon, M. A., Carpenter, D. E., Barratt, W. H., & Wilson, I. B. (1978) *Anal. Biochem. 85*, 519–527.
Grinvald, A., & Steinberg, I. Z. (1974) *Anal. Biochem. 59*, 583–598.
Grinvald, A., Schlessinger, J., Pecht, I., & Steinberg, I. Z. (1975) *Biochemistry 14*, 1921–1929.
Hazan, G., Grinvald, A., Maytal, M., & Steinberg, I. Z. (1974) *Rev. Sci. Instrum. 45*, 1602–1604.
Hobbiger, F. (1955) *Br. J. Pharmacol. 10*, 356–362.
Hovanec, J. W., & Lieske, C. N. (1972) *Biochemistry 11*, 1051–1056.
Hundley, L., Coburn, J., Garwin, E., & Stryer, L. (1967) *Rev. Sci. Instrum. 38*, 448–492.
Keijer, J. H., Worling, G. Z., & De Jong, L. P. A. (1974) *Biochim. Biophys. Acta 334*, 146–155.
Kirby, A. J., & Younas, M. (1970) *J. Chem. Soc. B*, 1165–1172.
Knopp, J., & Weber, G. (1969) *J. Biol. Chem. 244*, 6309–6315.
Lehrer, S. S., & Leavis, P. C. (1978) *Methods Enzymol. 49*, 222–236.
Loomis, A. T., & Salafsky, B. J. (1963) *Toxicol. Appl. Pharmacol. 5*, 685–701.
Lovejoy, C., Holowka, D. A., & Cathou, R. E. (1977) *Biochemistry 16*, 3668–3672.
Michel, O. H. (1958) *Fed. Proc., Fed. Am. Soc. Exp. Biol. 17*, 275.
Michel, O. H., Hackley, B. E., Berkowitz, L., List, G., Hackley, E. B., Gillman, W., & Pankau, M. (1967) *Arch. Biochem. Biophys. 121*, 29–33.
Monard, C., & Quinchon, J. (1961) *Bull. Soc. Chim. Fr.*, 1084–1086.
Pattison, S., & Bernhard, S. A. (1978) *Proc. Natl. Acad. Sci. U.S.A. 75*, 3613–3617.
Rosenberry, T. L. (1975) *Adv. Enzymol. Relat. Areas Mol. Biol. 43*, 103–218.
Rosenberry, T. L., Chang, H. W., & Chen, Y. T. (1972) *J. Biol. Chem. 247*, 1555–1565.
Saunders, B. C., & Stacey, G. J. (1948) *J. Chem. Soc.*, 695–699.
Schoene, K. (1978) *Biochim. Biophys. Acta 525*, 468–478.
Shinitzky, M., Dudai, Y., & Silman, I. (1973) *FEBS Lett. 30*, 125–128.
Sterri, S. H. (1977) *Biochem. Pharmacol. 26*, 656–658.
Stryer, L. (1968) *Science (Washington, D.C.) 162*, 526–533.
Sun, M., Chang, Z., Shau, M., Huang, R., & Chou, T. (1979) *Eur. J. Biochem. 100*, 527–530.
Tomlinson, G., Mutus, B., & McLennan, I. (1980) *Mol. Pharmacol. 18*, 33–39.
Turro, N. J. (1978) *Modern Molecular Photochemistry*, p 351, Benjamin/Cummings, New York.
Vaughn, W. M., & Weber, G. (1970) *Biochemistry 9*, 464–473.
Wilson, I. B., & Ginsburg, S. (1955) *Biochim. Biophys. Acta 18*, 168–170.
Wilson, I. B., & Rio, R. A. (1965) *Mol. Pharmacol. 1*, 60–65.
Wins, P., & Wilson, I. B. (1974) *Biochim. Biophys. Acta 334*, 137–145.